energies

MDPI

Article

Joint Prediction of the State of Charge and the State of Health of Lithium-Ion Batteries Based on the PSO-XGBoost Algorithm

Jiakun An [1], Wei Guo [1], Tingyan Lv [2,*], Ziheng Zhao [1], Chunguang He [1] and Hongshan Zhao [2]

1 State Grid Hebei Economic Research Institute, Shijiazhuang 050000, China
2 Department of Electric Power Engineering, North China Electric Power University, Baoding 071003, China
* Correspondence: lvtingyan_best@163.com

Abstract: Lithium-ion batteries are widely used in power grids as a common form of energy storage in power stations. The state of charge (SOC) and state of health (SOH) reflect the capacity and lifetime variation in the Li-ion batteries, and they are important state parameters of Li-ion batteries. Therefore, the establishment of accurate SOC and SOH prediction models is an essential prerequisite for the correct assessment of the status of lithium batteries, the improvement of the operational accuracy of energy-storage stations, and the development of maintenance plans for energy-storage stations. This paper first analyzes the correlation between SOC and SOH, and then proposes a joint SOC and SOH prediction model using the particle swarm optimization (PSO) algorithm to optimize the extreme gradient boosting algorithm (XGBoost), which takes into account the dynamic correlation between SOC and SOH dynamics, thus enabling more accurate SOC and SOH prediction. Finally, the prediction model is validated using the Oxford battery aging dataset. The correlation between SOC and SOH is verified by comparing the joint prediction results with the SOC individual prediction results. Then, the prediction results of the PSO-XGBoost model, the traditional XGBoost model, and the long short-term memory neural network are compared to verify the effectiveness and accuracy of the PSO-XGBoost model.

Keywords: lithium-ion battery; PSO-XGBoost; state of charge; state of health; joint prediction

check for updates

Citation: An, J.; Guo, W.; Lv, T.; Zhao, Z.; He, C.; Zhao, H. Joint Prediction of the State of Charge and the State of Health of Lithium-Ion Batteries Based on the PSO-XGBoost Algorithm. *Energies* **2023**, *16*, 4243. https://doi.org/10.3390/en16104243

Academic Editors: Daniel T. Hallinan, Jr., Ning Li, Linjing Zhang and Zhaoxia Peng

Received: 2 April 2023
Revised: 18 May 2023
Accepted: 19 May 2023
Published: 22 May 2023

1. Introduction

Due to their light weight, higher specific capacity, lower self-discharge rate, and longer cycle lifetime, lithium-ion batteries are commonly used as a form of energy storage in power grids. However, as lithium-ion batteries age, their internal resistance increases and their charge/discharge capacity decreases, leading to degradation of the performance of the energy-storage stations, low operational efficiency, and even the risk of thermal runaway and explosion. Therefore, it is necessary to predict the trend of the state of charge (SOC) and state of health (SOH) of Li-ion battery storage devices in the future cycle times in order to increase operational accuracy, control efficiency, and provide a basis for the next step of the operations and management plan. The SOC is the ratio of the current remaining capacity to the nominal capacity at a certain discharge rate and is an important parameter for lithium batteries [1] that quantifies the current energy left inside the battery, while the SOH is usually defined as the ratio of the decayed capacity to the nominal capacity and the ratio of the increased internal resistance to the initial internal resistance [2].

There is a large amount of research into SOC and SOH prediction, which can be divided into two main categories: model-based and data-driven. Model-based prediction methods for Li-ion batteries estimate the Li-ion battery state by means of an electrochemical model or an equivalent circuit model, combined with the established state-space equations. Wang Yuefei et al. first established the Randles equivalent circuit model to estimate the SOC from the open-circuit voltage measurements based on the SOC–OCV (open circuit voltage) curves under different SOHs [3,4]. In the literature [5], an improved ambient-temperature-dependent dual polarization model for lithium-ion batteries was developed and an extended Kalman filter (EKF) was proposed to estimate the SOC of lithium-ion batteries at different ambient temperatures. The literature [6] investigated the electrochemical impedance spectroscopy (EIS) of lithium-ion batteries under different states of charge and health, and used the support vector regression (SVR) method to develop an SOH estimation model for lithium-ion batteries to achieve the estimation of SOH. In the literature [7], a dual Kalman filter (KF)-type resilient filter was designed to estimate SOC in combination with a random missing measurement phenomenon modeled with a Bernoulli distributed sequence. The literature [8] established a second-order RC equivalent circuit model and built a state space based on the model, and then used an EKF to estimate the SOC. The data-driven approach establishes a mapping relationship between the state of the energy-storage device and the operational data by mining historical operational data without the need for state-space equations. It relies on direct data analysis and is more accurate [9]. The literature [10] used BP neural networks to learn the historical data of Li-ion batteries to establish the mapping relationship between SOC and the historical data. The literature [11] is based on a deep learning approach to estimate SOC. In the literature [12], an integrated framework of aging mechanisms and data-driven methods (IFAMDM) was developed for lithium-ion battery-accelerated aging diagnosis. Li Chaoran et al. proposed an SOC estimation model for Li-ion batteries based on a fusion of gated recurrent unit neural networks and Kalman filtering methods to achieve SOC prediction while reducing the impact of measurement errors and outliers on the results [13].

The above studies are all predictions for a single parameter and do not achieve a joint prediction of SOC and SOH. Current research on the joint prediction of SOC and SOH is mainly achieved by using the internal resistance parameter of the battery as a transition or by using deep learning methods.

The literature [14] used the unscented Kalman filter (UKF) to estimate SOC and identify the parameters within the state-space equation to obtain the internal resistance to estimate SOH. The literature [15] proposed a fast prediction method for battery SOC and SOH based on electrochemical impedance spectroscopy (EIS), but the method achieves SOH prediction using the SOC difference with the power obtained from short-time constant current discharge, and the prediction accuracy is difficult to guarantee. Wei Zhongbao et al. established an online adaptive equivalent circuit model to improve the accuracy of the model, established a capacity observer using the least-squares method and an SOC observer with a Kalman filter (KF) to build an SOC observer, and integrated a dual estimator to jointly estimate SOC and SOH [16]. In the literature [17], a combined charging voltage fragment and equivalent circuit model/data-driven fusion method was proposed for the SOC–SOH–RUL (remaining useful life) estimation framework for the joint estimation of SOC, SOH, and RUL over the long battery life cycle. In the literature [18], a gated recurrent unit recurrent neural network was combined with a convolutional neural network (CNN) using deep learning to achieve the joint estimation of SOC and SOH, which reduced the storage space requirement and improved the convergence speed. Liu Yunxin and Yao Liangzhong et al. exploited the temporal recurrence property of long short-term memory (LSTM) neural networks to achieve the joint prediction of SOC and SOH [19]. Although the above joint prediction methods can achieve the joint prediction of SOC and SOH, there are problems, such as the difficulty in obtaining parameters, the model learning results cannot be corrected, and the prediction accuracy needs to be further improved.

To this end, this paper adopts the XGBoost model for joint SOC and SOH prediction research based on a data-driven approach without the need for transition parameters such as internal resistance; it uses a particle swarm optimization algorithm to optimize the number of iterations and the maximum depth and learning rate of the XGBoost model to modify the model to reach optimality and establish a PSO-XGBoost regression prediction model. Finally, using the Oxford battery aging dataset, the historical operating data of voltage, current, surface temperature, SOC, and SOH of Li-ion battery energy-storage devices are used as feature quantities to compare and validate the effectiveness and accuracy of the proposed method in this paper, which provides new references and bases for the subsequent formulation of operation, maintenance, and overhaul plans for Li-ion battery energy-storage devices. The main research goal of this paper is to achieve the joint prediction of SOC and SOH parameters of lithium-ion batteries using the optimized XGBoost algorithm to further improve the prediction accuracy of the SOC of lithium batteries.

2. Correlation Analysis between SOC and SOH of Lithium-Ion Batteries

In order to ensure the safe and efficient operation of Li-ion batteries, the battery management system monitors Li-ion battery SOC and SOH as key state quantities, and there is a coupling relationship between them. As can be seen from the literature [20], both lithium-ion battery SOC and SOH are defined quantities that represent the state of the lithium-ion battery rather than specific physical quantities. According to the introduction of lithium-ion battery SOC in the literature [21], it is defined as the ratio of the current stored power of the battery to the current maximum available capacity of the battery; according to the introduction of lithium-ion battery SOH in the literature [22], the SOH can be defined from the perspective of capacity, which is the ratio of the current maximum available capacity of the battery to the nominal capacity. From the above analysis, it can be deduced that:

$$\mathrm{SOC}_1 = \frac{Q_0}{Q_N} \tag{1}$$

$$\mathrm{SOH} = \frac{Q_{\max}}{Q_N} \tag{2}$$

$$\mathrm{SOC}_2 = \frac{Q_0}{Q_N \cdot \mathrm{SOH}} \tag{3}$$

where Q_0 is the charge stored in the current state of the lithium-ion battery; Q_N is the nominal capacity of the lithium-ion battery; Q_{max} is the current maximum available capacity of the battery; SOC_1 indicates the state of charge without a consideration of battery aging, and SOC_2 indicates the state of charge with a consideration of battery aging. From Equation (3), it can be seen that there is a correlation between the SOC and SOH of the Li-ion batteries from the perspective of mechanistic analysis. In order to analyze the correlation between the two, and by analyzing the Oxford battery degradation dataset [23], it was possible to obtain a minimum value of SOH of approximately 75.7% for normal charging/discharging of Li-ion batteries. This paper studies the SOC curves of Li-ion battery storage devices when the battery is at the highest aging level, and the single charge/discharge cycle takes into account the different degrees of SOH influence, as shown in Figure 1.

As can be seen from Figure 1, the curve without considering the effect of SOH indicates that the maximum capacity of the Li-ion battery taken is the nominal capacity of the Li-ion battery, resulting in the predicted Li-ion battery SOC not reaching 100% at full charge. When the effect of the SOH is considered, the maximum capacity of the Li-ion battery can be more accurately obtained, the effect of SOH on SOC increases as the SOH decreases, and the full-charge SOC reaches 100% at an SOH of 75.7%. With the above analysis in Figure 1, there is a large coupling between the SOC and SOH in terms of both mechanism and perspective, so it is necessary to predict SOC and SOH jointly.

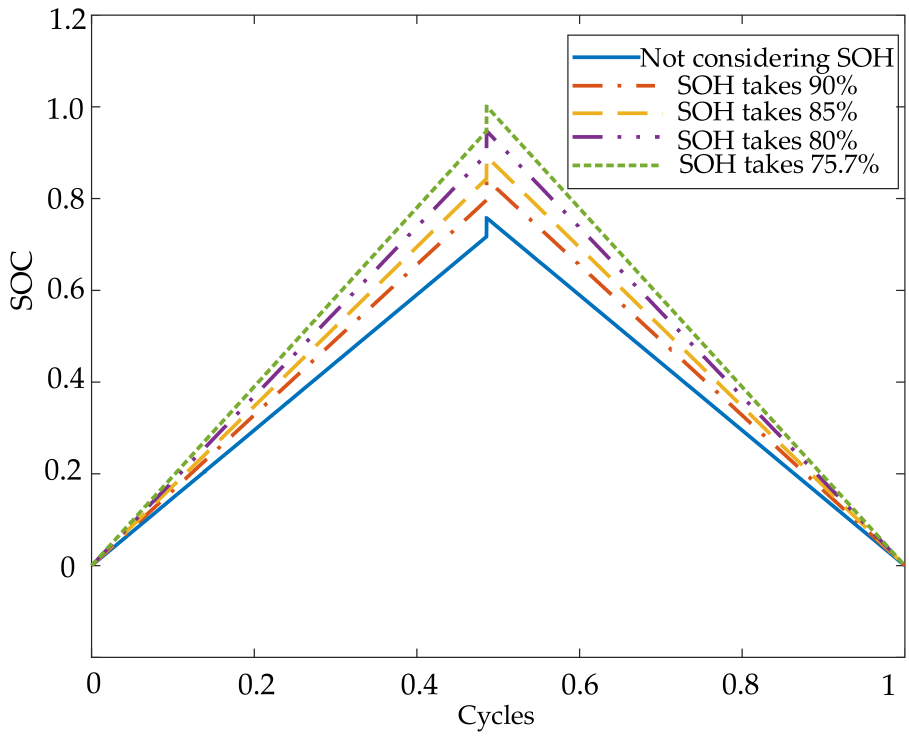

Figure 1. SOC variation curve of lithium-ion battery energy storage device.

3. A Joint SOC and SOH Prediction Model Based on the PSO-XGBoost Algorithm

3.1. XGBoost Algorithm

XGBoost (extreme gradient boosting) is an efficient and improved algorithm based on the GBRT (gradient boosting decision tree), which is both a linear scale solver and a decision tree learning algorithm. Compared with the traditional boosting library, the XGBoost algorithm performs a second-order Taylor expansion on the loss function and introduces two regularization terms, L_1 and L_2, to find the overall optimal solution, which measures the decline of the objective function and the overall complexity of the model, effectively improving the generalization ability of the model [24,25].

Assume that the experimental dataset used for the lithium-ion battery parameter prediction is denoted by E, $E = \{(\alpha_i, \beta_i) : i = 1, 2, \cdots, n, \alpha_i \in R^p, \beta_i \in R\}$. It consists of p features (including voltage, current, temperature, charge, etc.), for a total of n samples. Assuming that given *m (m = 1,2, . . . ,M)* regression trees and that G is the set space of the regression trees, the model can be expressed as:

$$\hat{\beta}_i = \sum_{m=1}^{M} f_m \alpha_i, f_m \in G \tag{4}$$

The objective function is:

$$f_{Obj} = \sum_{i=1}^{n} l\left(\beta_i, \hat{\beta}_i\right) + \sum_{m=1}^{M} \Omega(f_m) \tag{5}$$

where $\hat{\beta}_i$ is the predicted value; β_i is the true value; l is a differentiable convex loss function that measures the difference between the predicted and actual values; and $\Omega(f_m)$ is a regular term that is added to the XGBoost model to prevent over-fitting.

XGBoost uses the gradient boosting method of iterative operations, and a new regression tree is added to the model at each iteration, so that the result of the iteration at the t time is:

$$\hat{\beta}_i^{(t)} = \sum_{j=1}^{t} f_m(\alpha_i) = \hat{\beta}_i^{(t-1)} + f_t(\alpha_i) \tag{6}$$

Substituting Equation (6) into Equation (5), the objective function for the iteration at the t time is obtained as $Obj^{(t)}$:

$$f_{Obj}{}^{(t)} = \sum_{i=1}^{n} l\left[\beta_i, \hat{\beta}_i^{(t-1)} + f_t(\alpha_i)\right] + \Omega(f_m) + \sigma \tag{7}$$

The objective function is a second-order Taylor expansion with a canonical term $\Omega(f_m)$:

$$\begin{cases} f_{Obj}{}^{(t)} \cong \sum\limits_{i=1}^{n} \begin{bmatrix} \partial_{\hat{\beta}_i(t-1)} l\left(\beta_i, \hat{\beta}_i^{(t-1)}\right) f_t(\alpha_i) + \frac{1}{2}\partial^2_{\hat{\beta}_i(t-1)} l\left(\beta_i, \hat{\beta}_i^{(t-1)}\right) f_t^2(\alpha_i) \\ +\Omega(f_m) + \sigma \end{bmatrix} \\ \Omega(f_m) = \varphi H + \frac{1}{2}\delta\left\|\eta^2\right\| \end{cases} \tag{8}$$

where η and H are the leaf weight values and the number of tree leaf nodes, respectively; φ is the leaf tree penalty factor; δ is the leaf weight penalty factor; and σ is a constant due to the iteration of the objective function.

3.2. Particle Swarm Optimization Algorithm

In the particle swarm optimization algorithm, each solution corresponds to a particle in the search space, and each particle is an individual, consisting of a position vector and a velocity vector [26]. Assuming a population of u particles in a B-dimensional search space, the optimal position d_{best} generated by the particles in motion is denoted as:

$$d_i = (d_{i1}, d_{i2}, d_{i3}, \cdots, d_{iB}), i = 1, 2, \cdots, u \tag{9}$$

where B is the dimension of the particles and u is the number of particles.

The B-dimensional position vector of the i-th particle is noted as: $\lambda_i = (\lambda_{i1}, \lambda_{i2}, \lambda_{i3}, \cdots, \lambda_{iB})$, and the velocity vector of the i-th particle is noted as: $\varepsilon_i = (\varepsilon_{i1}, \varepsilon_{i2}, \varepsilon_{i3}, \cdots, \varepsilon_{iB})$. These two determine the position and direction of flight of the i-th particle, respectively. $d_g = \left(d_{g1}, d_{g2}, d_{g3}, \cdots, d_{gB}\right)$ is the optimal position searched for throughout the particle swarm history, where g is the particle number, $g \in \{1, 2, \cdots, u\}$.

The particle swarm optimization algorithm first initializes the swarm of particles, calculates the fitness value of each particle, and searches for the optimal solution through iterations. In each iteration, the particles update their velocities and positions by means of individual and global extremes, with the following update formula:

$$\begin{cases} \varepsilon_i^{c+1} = \tau\varepsilon_i^c + q_1 s_1 \left(d_i^c - \lambda_i^c\right) + q_2 s_2 \left(d_g^c - \lambda_g^c\right) \\ \lambda_i^{c+1} = \lambda_i^c + \varepsilon_i^{c+1}, (i = 1, 2, \cdots, u) \end{cases} \tag{10}$$

where c is the number of iterations; τ is the inertia weight; s_1, s_2 is a random number between [0, 1]; and q_1, q_2 is the acceleration factor, also called the learning factor.

3.3. Joint SOC and SOH Prediction Model Building

Based on the XGBoost principle and the PSO algorithm theory, a joint prediction model of SOC and SOH for lithium batteries with PSO-optimized XGBoost parameters is constructed, as shown in Figure 2.

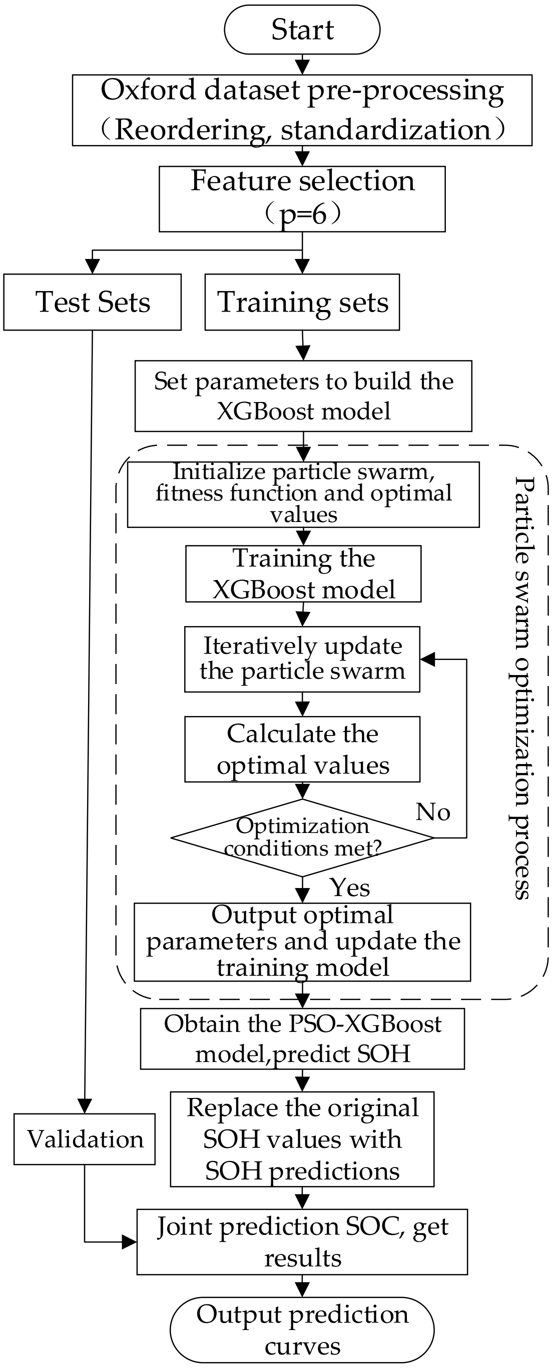

Figure 2. Lithium-ion battery SOC and SOH joint prediction model flow chart.

As can be seen from Figure 2, the process for the joint prediction of the model developed is as follows:

(1) Data preprocessing: remove missing values from the dataset, reorder and normalize them.
(2) Use "SOC" and "SOH" as output features and the remaining features as input; use 70% of the dataset as training set and 30% as test set.
(3) Initialize the particles and their velocities, set the random sampling rate (subsample) and the minimum leaf node sample weight (min_child_weight) as the parameters to be sought, set the coefficient of determination of the model fit as the value of the fitness function, and initialize the global optimum and the individual optimum of the particles according to the value of the fitness function.

(4) Update the particle velocity and position according to Equation (10), calculate its fitness value, and update the individual optimal value and the global optimal value.
(5) Determine whether the stopping condition is satisfied; if not, the individual optimum and the global optimum will continue to be updated. If satisfied, the optimum parameters will be output (subsample, min_child_weight).
(6) Select the optimal combination of parameters (subsample, min_child_weight) and construct the XGBoost regression model with parameter optimization.

4. Validation Analysis

In order to validate the joint prediction model proposed in this paper, experiments were conducted based on the Oxford battery degradation dataset [21]. Firstly, the SOC was predicted individually, and the individual prediction was compared with the joint prediction to verify the correlation between SOC and SOH and the significance of the joint prediction; then, two sets of comparison experiments were conducted. Comparison experiment 1 was a lithium battery prediction method using the traditional XGBoost model, and comparison experiment 2 was a lithium battery prediction method based on LSTM (long short-term memory). Their prediction results were compared with the prediction results of this paper to verify the accuracy of the joint prediction model proposed in this paper.

4.1. Experiment Data

The Oxford battery aging dataset was obtained from eight Kokam lithium-ion cobalt-acid batteries with a rated capacity of 740 mAh. All data in the Oxford battery aging dataset were tested under ARTEMIS [27] urban driving conditions at a constant temperature of 40 °C, obtained after constant current charge and discharge cycles of 1.48 A (2C) on the Li-ion battery. The data recorded in this dataset include voltage, current, temperature, charge, and other Li-ion battery data; 8200 charge/discharge cycles were recorded for each battery, and data were measured every 100 cycles, with 5000–6000 data points recorded each time, ultimately enabling approximately 150,000 data points to be sampled. All of these data can be used to predict the SOC. However, the SOH has a larger time scale and longer time interval than the SOC parameters, generally in days, and the cycle time of the batteries in the dataset is about 500–600 days, while some of the non-compliant data and null values in the dataset were deleted. The final result is a total of 517 charge/discharge curves that can be used for SOH prediction. In this paper, the data from the cyclic charging and discharging process of Li-ion battery No. 1 were taken as a sample; the data were first reordered in the order of charging and discharging time, and then the features ($p = 6$) selected in the joint prediction model were determined, which are temperature, charge, SOH value, voltage, moment, and SOC measured value. The training and test sets were divided in a ratio of 7:3. The PSO algorithm was used to optimize the three parameters of the number of iterations, the maximum depth, and the learning rate for each feature quantity. At the same time, in order to eliminate the effects of different orders of magnitude as well as units between different features and to improve the convergence of the model, Equation (11) was adopted to normalize the input and output data so that the individual feature sequences were compressed between [0, 1].

$$x_i^* = \frac{x_i - x_{\min}}{x_{\max} - x_{\min}} \tag{11}$$

where $x_{\max}$ is the highest value in the feature series; $x_{\min}$ is the lowest value in the feature series; x_i^* is the normalized value of the feature series; and x_i is the initial value of the feature series.

4.2. Predicted Results

To verify the validity of the PSO-XGBoost model, the Li-ion battery voltage and temperature were first predicted. The prediction results are the future cycle voltage versus temperature curves. To see how well the model predicts, the prediction curves were locally scaled up. This is shown in Figures 3 and 4.

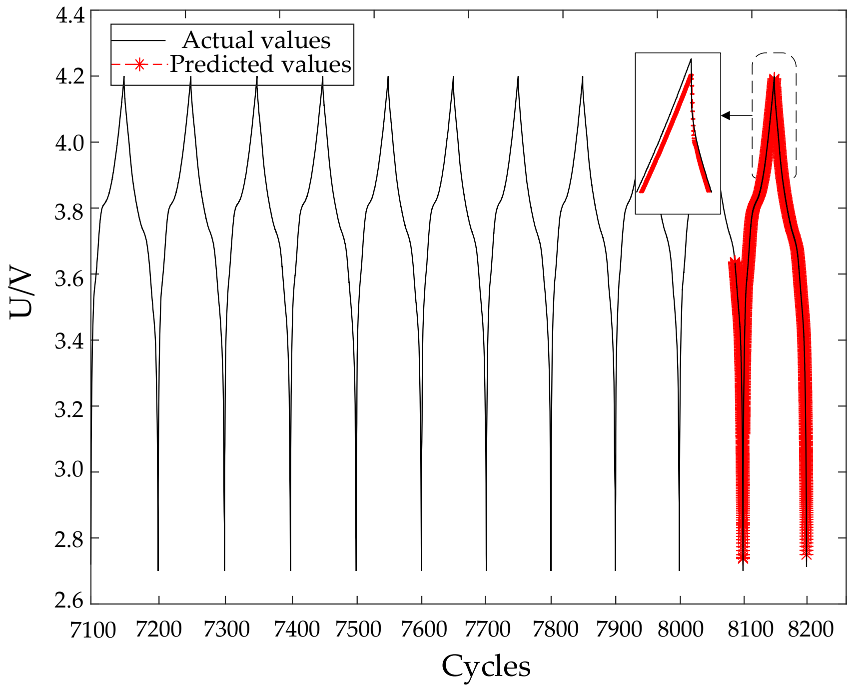

Figure 3. Lithium-ion battery voltage prediction curve.

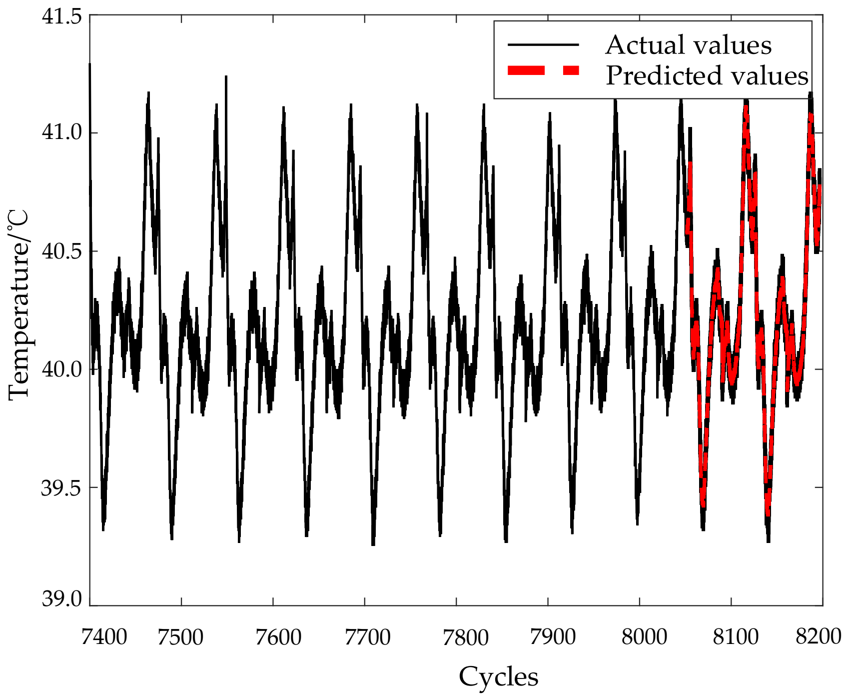

Figure 4. Lithium-ion battery temperature prediction curve.

As can be seen from Figures 3 and 4, the predicted results of the PSO-XGBoost model are very close to the actual values. In Figure 3, the maximum difference between the predicted and true values of the voltage is about 0.01 V; in Figure 4, the maximum difference between the predicted and true values of temperature is about 0.08 °C. This demonstrates the feasibility of the model proposed in this paper when used for voltage and temperature prediction, and also lays the foundation for the accurate prediction of SOC values later on.

To verify the accuracy of the proposed joint SOC and SOH prediction method, the PSO-XGBoost model was used first to predict the SOH based on the Oxford aging dataset, followed by a joint prediction of SOC and SOH, and then compared with SOC alone. The SOH prediction curve for Li-ion batteries is shown in Figure 5, the joint prediction curve of SOC and SOH for Li-ion batteries is shown in Figure 6, and the comparison results between the joint prediction and the prediction when only SOC is considered are shown in Figure 7.

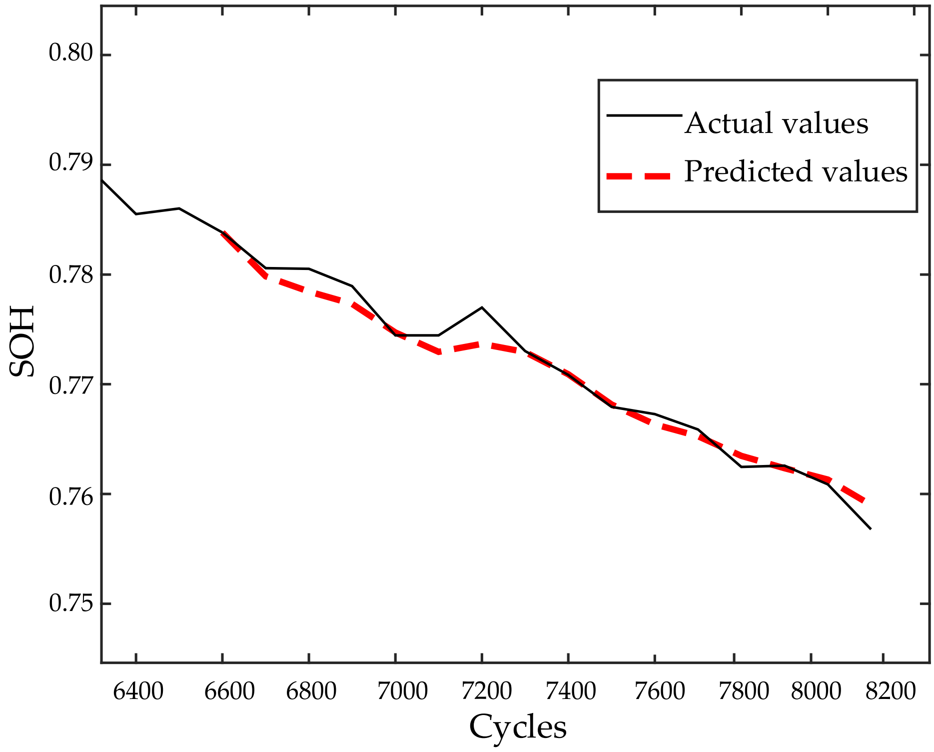

Figure 5. Lithium-ion battery SOH prediction curve.

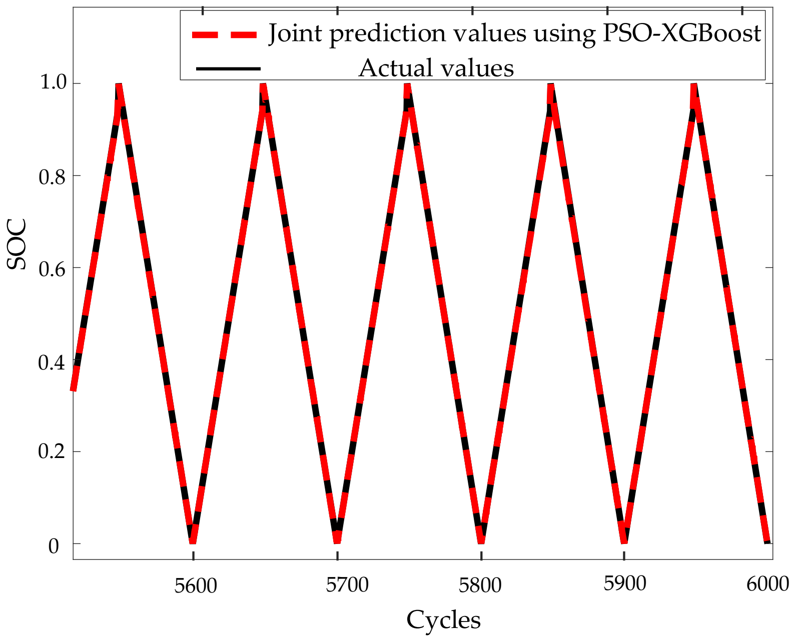

Figure 6. Joint Prediction curve for lithium-ion batteries.

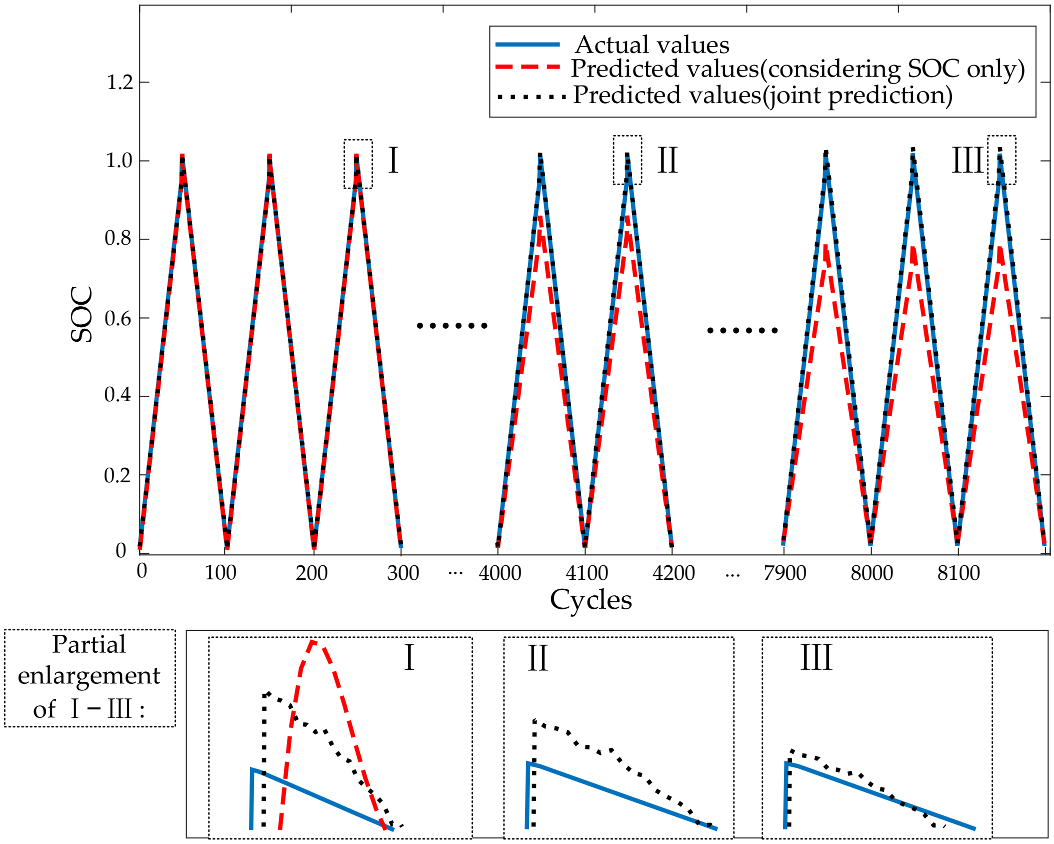

Figure 7. Joint prediction versus individual forecasts.

As can be seen from Figure 5, the SOH value of the lithium battery gradually decreases as the number of cycles increases, reaching a minimum of about 0.757 at the last cycle (8200 cycles). It is also verified that the method proposed in this paper can predict the trend of the SOH of Li-ion batteries more accurately, and the maximum difference between the predicted value and the real value is only about 0.03.

As can be seen from Figure 6, the method proposed in this paper can predict the trend of the lithium battery SOC very accurately, and the accuracy is higher than that in Figure 5 when predicting SOH. The reason for this is that the battery SOC parameter is influenced by the battery SOH, but the SOH parameter is mainly influenced by factors related to battery usage time, etc., and is relatively less influenced by SOC. This also validates the correctness of the SOC–SOH correlation analysis for lithium-ion batteries in Section 2 of this paper.

According to the partial enlargement of Figure 7, it can be seen that the joint prediction method of SOC and SOH proposed in this paper has a higher accuracy than when the SOC is predicted separately. From the analysis in Section 1, it is clear that the actual capacity decays with increasing age. The prediction method proposed in this paper can predict the change trend of the SOH in the subsequent charging/discharging cycles based on the aging law and use the SOH prediction value as the input for predicting SOC, so it can predict the SOC curve more accurately; the method considering only the SOC prediction does not consider the influence of the aging factor.

4.3. Comparison of Prediction Results of Different Methods

Based on the Oxford battery aging dataset, three methods, the PSO-XGBoost model, the traditional XGBoost model, and the LSTM neural network model, were used for the joint prediction of SOC and SOH. The prediction results of SOC are shown in Figure 8.

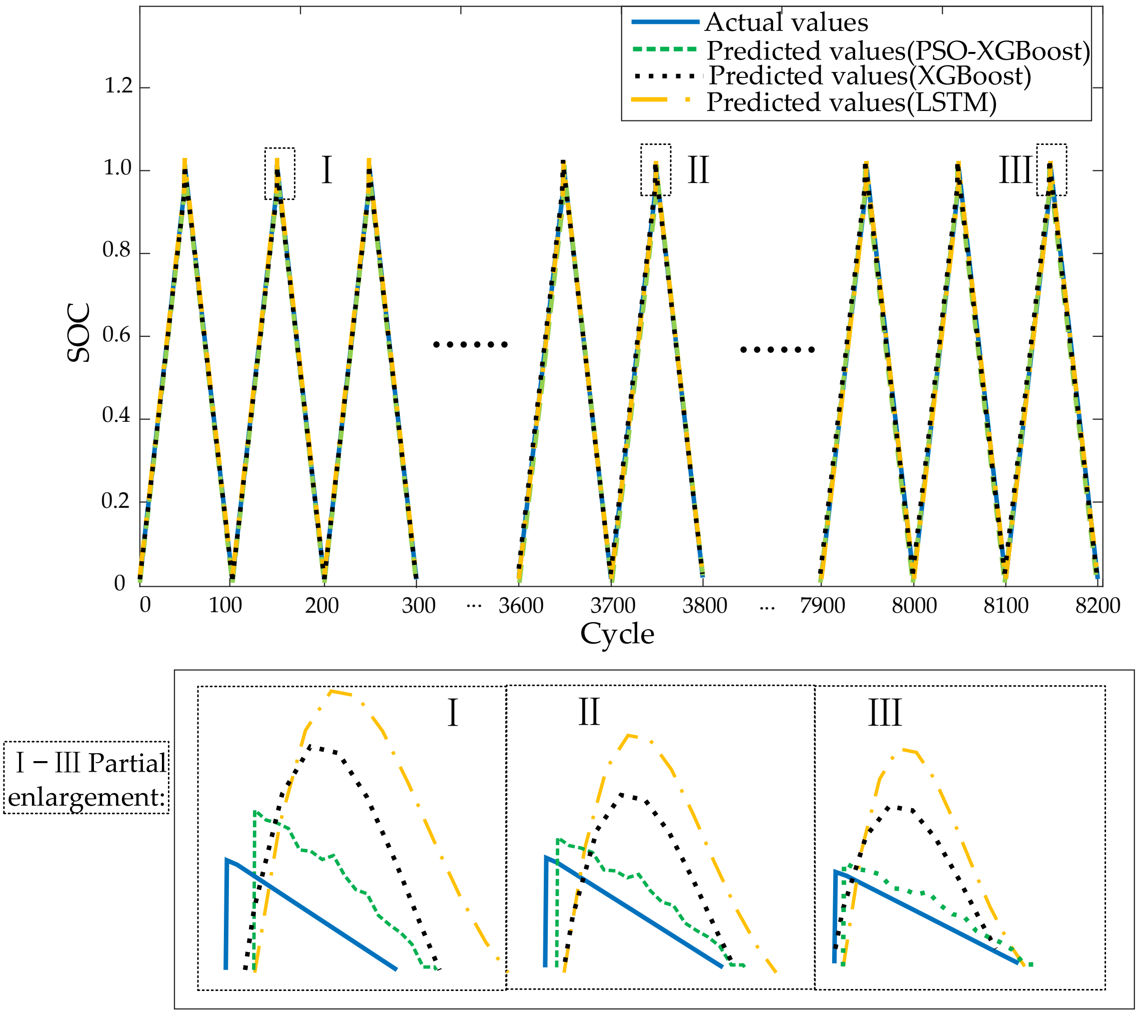

Figure 8. Joint prediction of SOC curves using different methods.

As can be seen from the partial enlargement of Figure 8, the combined SOC and SOH prediction method proposed in this paper is more accurate, and the prediction curves fit the actual values more closely, than other methods, and the accuracy of the predicted SOC is higher than other methods. Meanwhile, comparing the prediction results in Figure 6 with the prediction results of the PSO-XGBoost method in Figure 8, it can be seen that the proposed method in this paper has good prediction accuracy for different numbers of cycles.

In order to more intuitively analyze the accuracy of the proposed prediction method when used for the joint prediction of SOC and SOH, two error evaluation indicators are defined in this paper, namely, mean absolute error (MAE) and root-mean-square error (RMSE), as shown in Equations (12) and (13):

$$E_{\mathrm{MAE}} = \frac{1}{N}\sum_{t=1}^{N}|y_t - \hat{y}_t| \tag{12}$$

$$E_{\mathrm{RMSE}} = \sqrt{\frac{1}{N}\sum_{t=1}^{N}(y_t - \hat{y}_t)^2} \tag{13}$$

where y_t is the true value of the lithium battery state quantity at moment t.

The joint prediction error analysis of this paper's method with other methods using the above two evaluation indicators is shown in Table 1.

Table 1. RMSE and MAE of different prediction models.

Predicted Objects	Methods	MAE/%	RMSE/%
SOC	PSO-XGBoost	0.184	0.192
	XGBoost	0.342	0.358
	LSTM	0.62	0.74
SOH	PSO-XGBoost	0.197	0.214
	XGBoost	0.36	0.379
	LSTM	0.51	0.62

As can be seen from Table 1, the joint SOC and SOH prediction method proposed in this paper can show better performance, with the MAE and RMSE of the proposed prediction model for the SOH prediction being 0.197% and 0.214%, respectively, and the MAE and RMSE of the achieved SOC prediction being 0.184% and 0.192%, respectively. They are all lower than the other models. The error data is plotted as a radar plot, as shown in Figure 9.

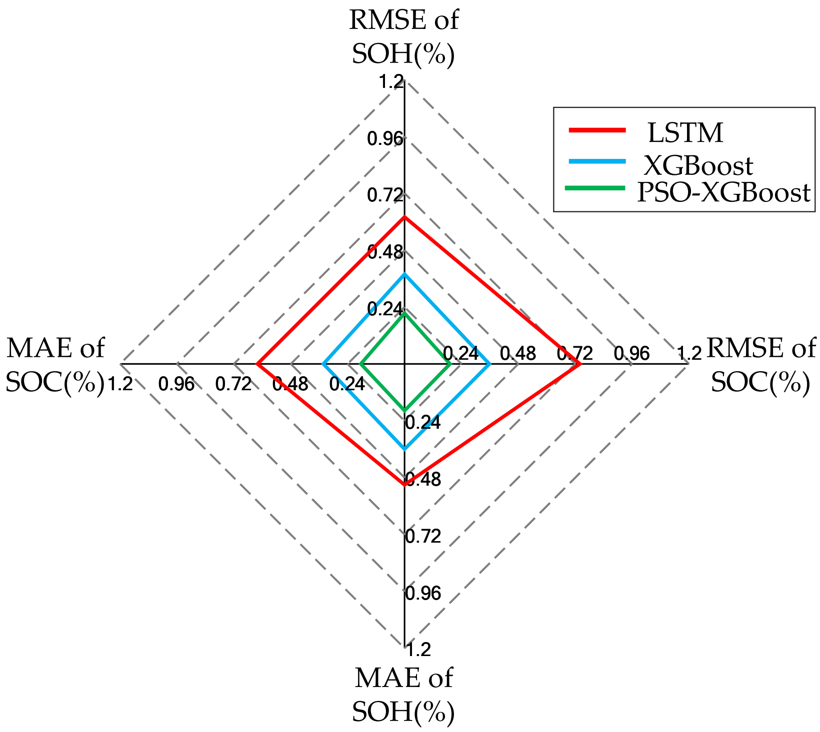

Figure 9. RMSE and MAE radar plots for different models.

It is also more clearly seen from Figure 9 that the PSO-XGBoost method proposed in this paper has a smaller enclosing area in the error radar plot. Therefore, the method in this paper can improve the accuracy of SOC prediction and achieve the joint prediction of SOC and SOH with high accuracy. As can be seen from Figure 7, the joint prediction accuracy of the model proposed in this paper is significantly higher than that of SOC alone. In summary, the effectiveness and accuracy of the joint SOC and SOH prediction method based on the PSO-XGBoost model proposed in this paper has been verified.

5. Conclusions

(1) In order to improve the joint prediction accuracy of the SOC and SOH of Li-ion battery energy-storage devices, a more accurate PSO-XGBoost model for joint prediction of the SOC and SOH of Li-ion batteries is proposed in this paper by combining the PSO algorithm and the XGBoost algorithm.

(2) The analysis of the experimental results based on the Oxford battery aging dataset shows that the PSO-XGBoost model proposed in this paper achieves not only the prediction of the lithium battery temperature and voltage, but also the joint prediction of the SOC and SOH with higher accuracy than of the SOC alone, verifying the correlation between SOC and SOH.
(3) To verify the accuracy of the PSO-XGBoost model, the PSO-XGBoost model, the XGBoost model, and LSTM neural networks were applied to Li-ion battery SOC and SOH prediction. The results show that the RMSE and MAE of the SOC and SOH prediction results of the PSO-XGBoost model proposed in this paper are lower than those of the traditional XGBoost model and the LSTM neural network, so the method proposed in this paper achieves more accurate joint prediction of the SOC and SOH of Li-ion battery energy-storage devices.

Author Contributions: For Methodology, J.A. and T.L.; writing—original draft, T.L. and W.G.; writing—review and editing, Z.Z. and C.H.; data curation, T.L. and H.Z. All authors have read and agreed to the published version of the manuscript.

Funding: This work is supported by a project of the State Grid Hebei Economic Research Institute (SGHEJY00GHJS2200055).

Data Availability Statement: Not applicable.

Conflicts of Interest: The authors declare no conflict of interest.

References

1. Huang, J.; Li, J.L.; Li, Z. A state of health rapid assessment method for decommissioned lithium-ion batteries. *Power Syst. Prot. Control* **2021**, *49*, 25–32. (In Chinese) [CrossRef]
2. Li, C.; Wang, C.H.; Wang, G.; Lu, Z.H.; Ma, C.Z. Review on implementation method analysis and performance comparison of lithium battery state of charge estimation. *Energy Storage Sci. Technol.* **2022**, *11*, 3328–3344. [CrossRef]
3. Wang, Y.F.; Huang, L.; Shu, C.C.; Zhang, N.; Xia, J.B. Research on SOC and SOH estimation of vehicle lead-acid battery. *Agricult. Equip. Veh. Eng.* **2017**, *55*, 19–24. (In Chinese)
4. Shu, C.C. Research on the Co-Estimation of SOC and SOH and on Charging-Discharging Strategy of the Vehicular Lead-Acid Battery. Master's Thesis, Hefei University of Technology, Hefei, China, 2018.
5. Pang, H.; Guo, L.; Wu, L.X.; Jin, J.M.; Liu, K. An improved dual polarization model of Li-ion battery and its state of charge estimation considering ambient temperature. *Trans. China Elect. Soc.* **2021**, *36*, 2178–2189. (In Chinese) [CrossRef]
6. Fan, M.S.; Geng, M.M.; Yang, K.; Zhang, M.; Liu, H. State of Health Estimation of Lithium-Ion Battery Based on Electrochemical Impedance Spectroscopy. *Energies* **2023**, *16*, 3393. [CrossRef]
7. Peng, Z.X.; Pan, C.Y.; Yang, S.C.; Wen, G.G.; Huang, T. Resilient Filter for State of Charge and Parameter Co-estimation with Missing Measurement. *IEEE Trans. Indust. Inform.* **2022**, 1–10. [CrossRef]
8. Shen, P.; Ouyang, M.G.; Lu, L.G.; Li, J.; Feng, X. The co-estimation of state of charge, state of health, and state of function for lithium-ion batteries in electric vehicles. *IEEE Trans. Veh. Technol.* **2018**, *67*, 92–103. [CrossRef]
9. Zhang, M.; Yang, D.F.; Du, J.X.; Sun, H.; Li, L.; Wang, L.; Wang, K. A Review of SOH Prediction of Li-Ion Batteries Based on Data-Driven Algorithms. *Energies* **2023**, *16*, 3167. [CrossRef]
10. Zhao, Z.K.; Han, X.J.; Ma, H.M. Capacity fade prediction model of battery energy storage system based on BP neural network. *Electrical. Energy Manag. Technol.* **2016**, *19*, 68–72. (In Chinese) [CrossRef]
11. Jiménez-bermejo, D.; Fraile-ardanuy, J.; Castaño, S.; Merino, J.; Álvaro-Hermana, R. Using dynamic neural networks for battery state of charge estimation in electric vehicles. *Procedia Comp. Sci.* **2018**, *130*, 533–540. [CrossRef]
12. Jia, X.Y.; Zhang, C.P.; Wang, L.Y.; Zhang, L.; Zhou, X. Early Diagnosis of Accelerated Aging for Lithium-Ion Batteries with an Integrated Framework of Aging Mechanisms and Data-Driven Methods. *IEEE Trans. Transp. Elect.* **2022**, *8*, 4722–4742. [CrossRef]
13. Li, C.R.; Xiao, F.; Fan, Y.X.; Yang, G.R.; Tang, X. A hybrid approach to lithium-ion battery SOC estimation based on recurrent neural network with gated recurrent unit and Huber-M robust Kalman filter. *Trans. China Elect. Soc.* **2020**, *35*, 2051–2062. (In Chinese) [CrossRef]
14. Jiang, C. Joint Online Estimation of SOC and SOH for Lithium-Ion Battery Based on Improved Dual Kalman Filtering. Master's Thesis, Southwest University of Science and Technology, Mianyang, China, May 2021.
15. Luo, F.; Huang, H.H.; Wang, H.X. Rapid prediction of the state of charge and state of health of decommissioned power batteries based on electrochemical impedance spectroscopy. *Chin. J. Sci. Instrum.* **2021**, *42*, 172–180. [CrossRef]
16. Wei, Z.B.; Zhao, J.Y.; Ji, D.X.; Tseng, K.J. A multi-timescale estimator for battery state of charge and capacity dual estimation based on an online identified model. *Appl. Energy* **2017**, *204*, 1264–1274. [CrossRef]

17. Zhang, J.A.; Wang, P.; Cheng, Z. A joint estimation framework of SOC-SOH-RUL for lithium batteries based on charging voltage segment and hybrid method. *Power Syst. Technol.* **2021**, *46*, 1063–1072. [CrossRef]
18. Li, C.R.; Xiao, F.; Fan, Y.X.; Tang, X.; Yang, G.R. Joint Estimation of the State of Charge and the State of Health Based on Deep Learning for Lithium-ion Batteries. *Proc. Csee* **2021**, *41*, 681–692. [CrossRef]
19. Liu, Y.X.; Yao, L.Z.; Zhou, J.H.; Chen, C.; Ke, D.; Liao, S.; Gong, L.; Cheng, F. Joint Prediction of State of Charge and State of Health Based on LSTM for Lithium-ion Batteries. *J. Glob. Energy Interconnect.* **2022**, *5*, 37–45. [CrossRef]
20. Zhu, L.Q.; Zhang, J.Q. A new model of jointed states of charge and health for lithium batteries. *Proc. Csee* **2018**, *38*, 3613–3620. [CrossRef]
21. Juan, R.B.; Nicolás, M.G.; Henry, S.M. SoC estimation for lithium-ion batteries: Review and future challenges. *Electronics* **2017**, *6*, 102. [CrossRef]
22. Pan, H.H.; Lü, Z.Q.; Wang, H.M.; Wei, H.; Chen, L. Novel battery state-of-health online estimation method using multiple health indicators and an extreme learning machine. *Energy* **2018**, *160*, 466–477. [CrossRef]
23. Birkl, C. Diagnosis and Prognosis of Degradation in Lithium-Ion Batteries. Master's Thesis, University of Oxford, Oxford, UK, 2017.
24. Qiu, C.M.; Wang, Q.J.; Xie, F.; Qian, Z. Prediction Method of Full-condition and High-precision Current of Asynchronous Motors for Electric Vehicles Based on XGBoost. *Proc. Csee* **2020**, *40*, 313–322. [CrossRef]
25. Zhao, H.S.; Yan, X.H.; Wang, G.L.; Yin, X.L. Fault Diagnosis of Wind Turbine Generator Based on Deep Autoencoder Network and XGBoos. *Autom Electr. Power Syst.* **2019**, *43*, 81–86. [CrossRef]
26. Wu, C.H.; Dong, A.L.; Li, Z.H.; Wang, F. Photovoltaic Power Prediction Based on Graph Similarity Day and PSO-XGBoost. *High Volt. Eng.* **2022**, *48*, 3250–3259. [CrossRef]
27. André, M. The ARTEMIS European driving cycles for measuring car pollutant emissions. *Sci. Total. Environ.* **2004**, *334–335*, 73–84. [CrossRef]